

# Results on Prompt Fission Gamma Rays with the STEFF detector at the n\_TOF facility

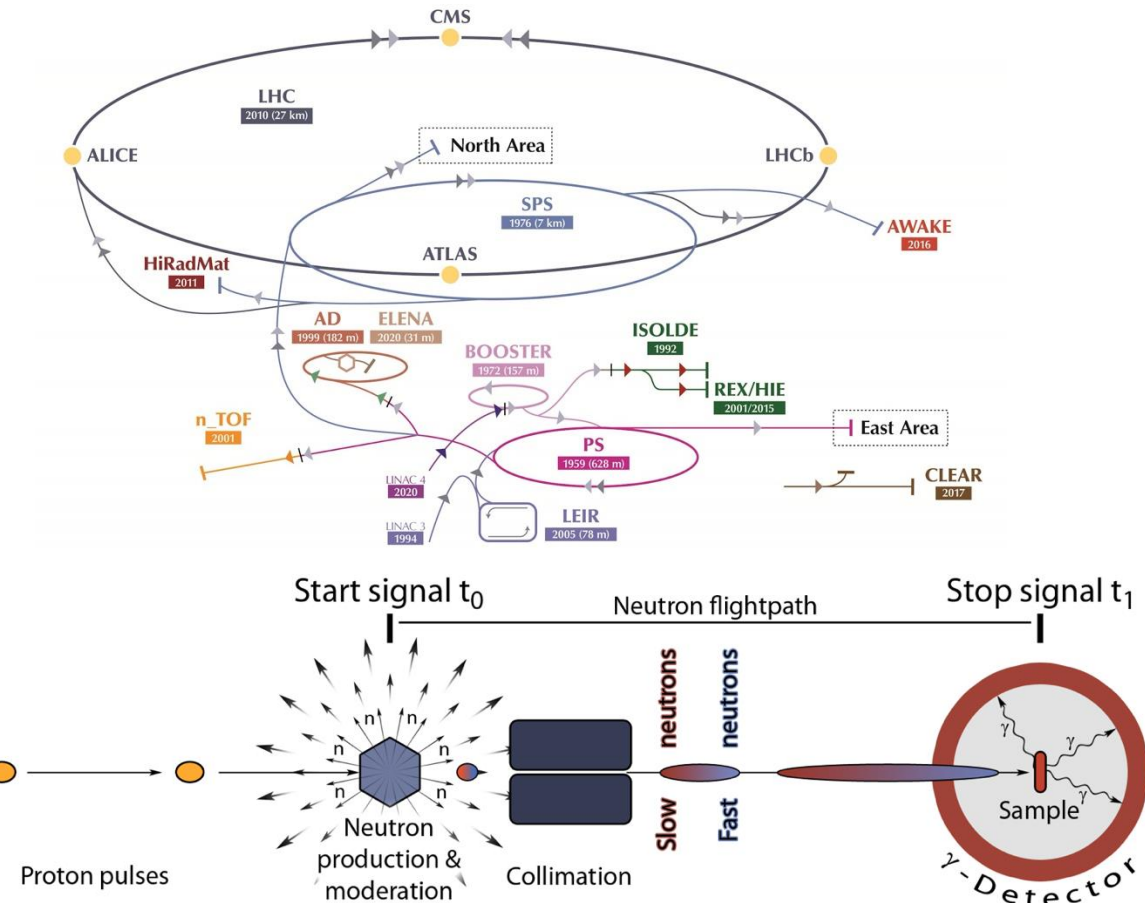


Dr Toby Wright  
Research Fellow

The University of Manchester



# What is n\_TOF



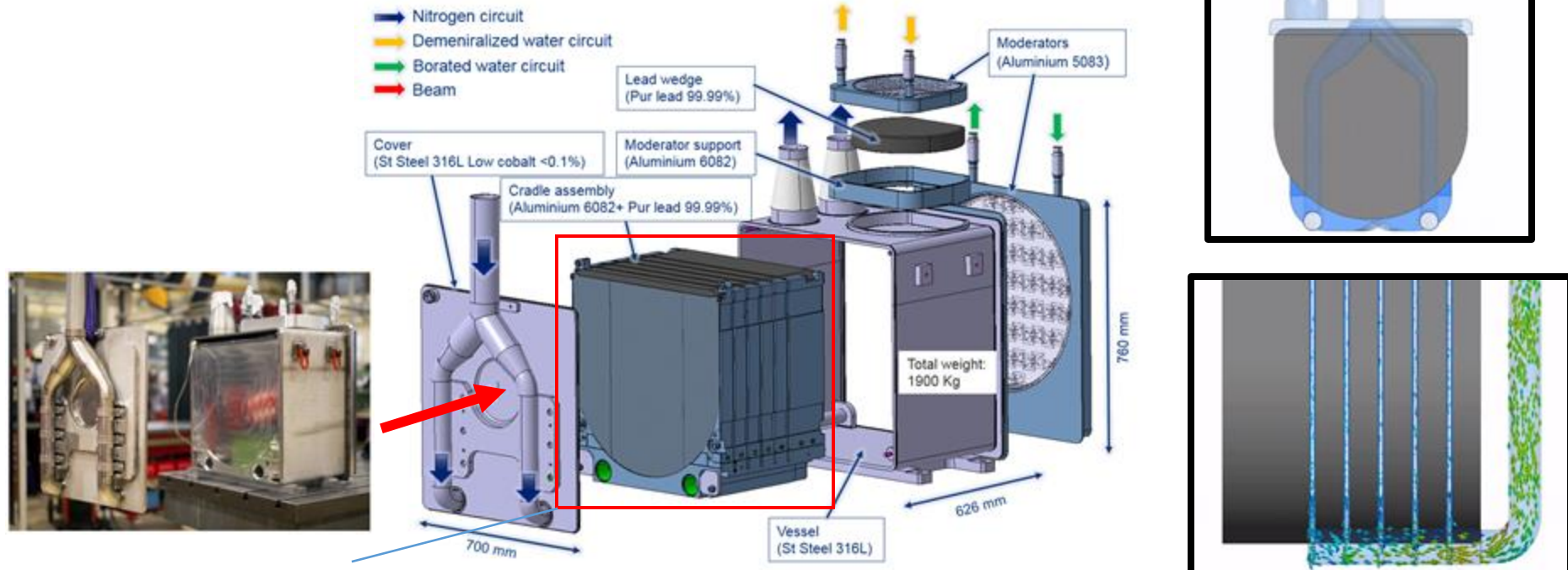
150 researchers  
40 research institutions/teams  
20 PhD students/year

n\_TOF Youtube



# The n\_TOF facility – 3<sup>rd</sup> generation target

- 20 GeV/c protons
- $8.5 \times 10^{12}$  protons/pulse
- Max repetition rate  $\sim 0.8$  Hz
- 7 ns rms pulse width
- 2 cm FWHM
- $\sim 2$  cm FWHM (capture mode)



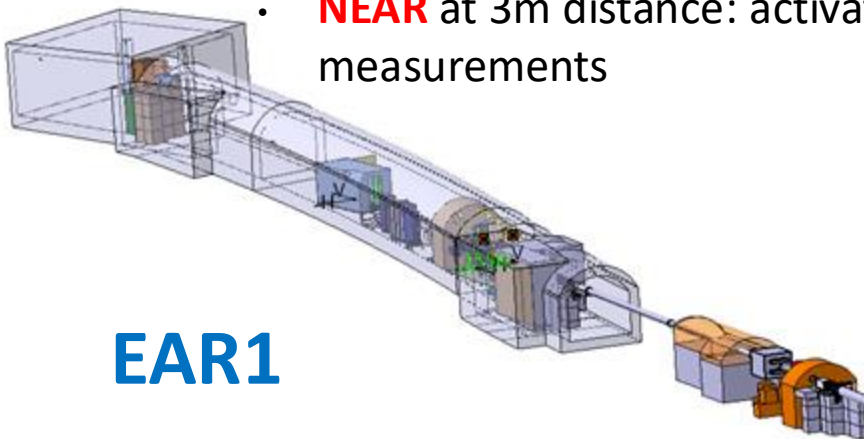
N<sub>2</sub> gas cooling to avoid Pb corrosion and contamination of the cooling circuit



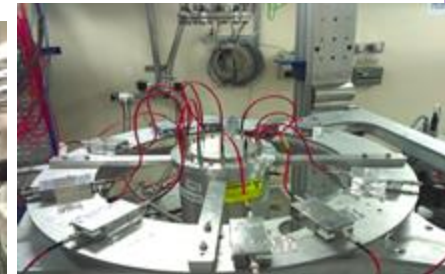
# The n\_TOF facility: EAR1 + EAR2 + NEAR

## Three experimental areas (EAR)

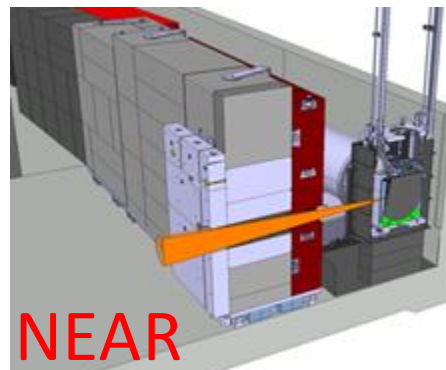
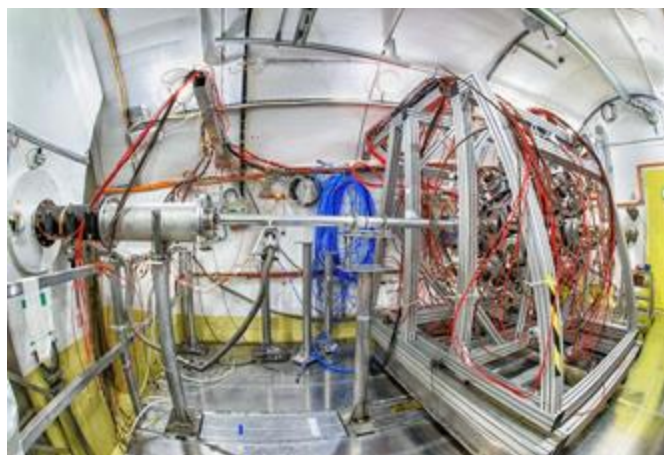
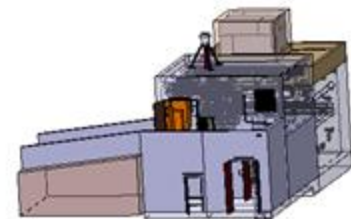
- Horizontal flight path: **EAR1** at 200 m
- Vertical flight-path: **EAR2** at 20 m
- **NEAR** at 3m distance: activation measurements



**EAR1**



**EAR2**

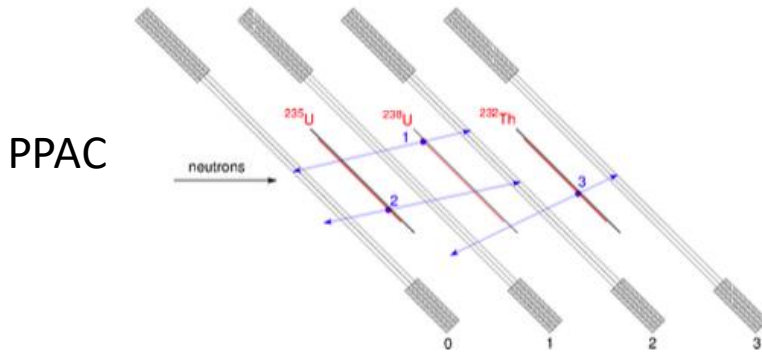


**NEAR**

Proton  
beam

# Fission at n\_TOF

N. Colonna et al., “The fission experimental programme at the CERN n TOF facility: status and perspectives”, *Eur. Phys. J. A* (2020) 56: 48



MicroMegas

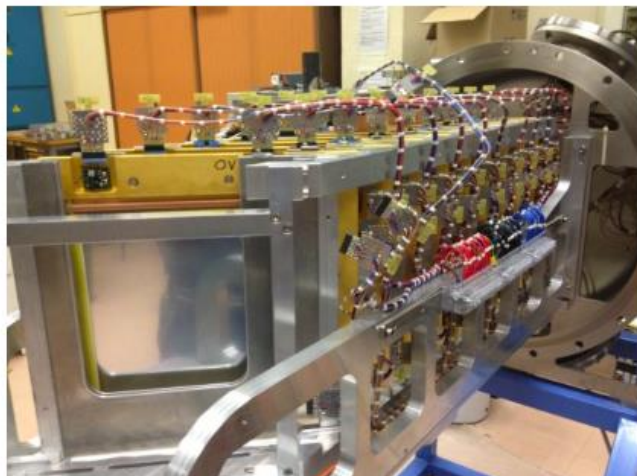


**Fig. 15.** PPAC and target assembly layout for Phase-II (top drawing). Ten detectors and nine samples are mounted in the scattering chamber tilted by  $45^\circ$  with respect to the neutron beam direction, as seen in the photograph. The sample holders are visible between the PPACs.

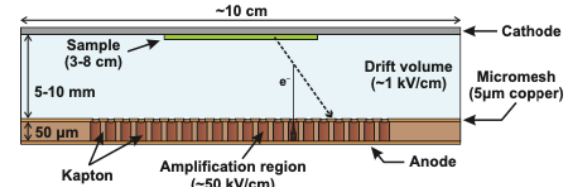


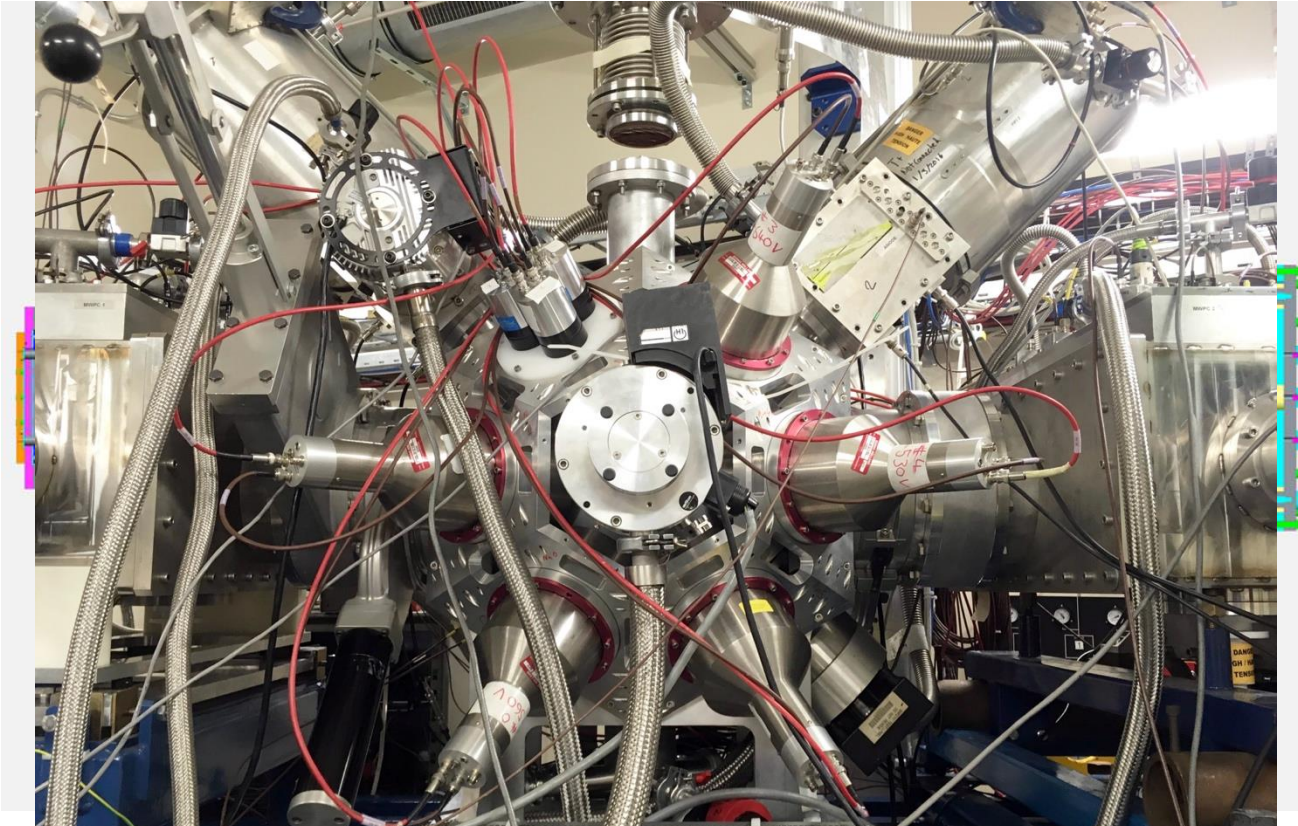
**Fig. 20.** An illustration of the basic principle of operation of a Micromegas detector (not to scale). An ionising particle (e.g. a fission fragment) ionises the gas in the drift region. The ionisation electrons drift towards the micromesh and are multiplied inside the amplification region, inducing a signal. Indicative values are given for the electrical field strengths and



**Fig. 23.** A setup consisting of ten Micromegas detectors, coupled with six  $^{241}\text{Am}$  samples and two  $^{235}\text{U}$  and  $^{238}\text{U}$  reference samples, before insertion into the chamber.

# STEFF

---



# Experimental Campaign and motivation



**100  $\mu\text{g}/\text{cm}^2$   $^{235}\text{U}$  target,  
81 mm diameter disc,  
0.7  $\mu\text{m}$  Al backing (CEA  
ORsay))**

- 2E2v measurement for fission yields
- Accurate measurement of the average energies and multiplicities of prompt fission  $\gamma$ -rays

Data Bank » Nuclear Data Services  
NEA Nuclear Data High Priority Request List

HPRL Main	High Priority Requests (HPR)	General Requests (GR)	Special Purpose Quantities (SPQ)		New Request	EG-HPRL (SG-C)				
			Standard	Dosimetry						
<b>Results of your search in the request list</b>										
Requests are shown from the following list(s): <b>High Priority (H)</b>										
ID	View	Target	Reaction	Quantity	Energy range	Sec.E/Angle				
2H		8-0-16	(n,el) / (n,abs)	SIG	2 MeV-20 MeV	See details				
2H		94-PU-239	(n,el)	prompt g	Thermal-Fast	Eg=0-10MeV				
2H		92-U-235	(n,el)	prompt g	Thermal-Fast	Eg=0-10MeV				
8H		1-H-2	(n,el)	DA/DE	0.1 MeV - MeV	0-180 Deg				
10H		10-H-2	(n,el)	DA/DE	0.1 MeV - MeV	0-180 Deg				

ELSEVIER

Nuclear Data Sheets 163 (2020) 261–279

[www.elsevier.com/locate/nds](http://www.elsevier.com/locate/nds)

## Evaluation of the Prompt Fission Gamma Properties for Neutron Induced Fission of $^{235}\text{U}$ , $^{238}\text{U}$ and $^{239}\text{Pu}$

I. Stetcu,<sup>1,\*</sup> M.B. Chadwick,<sup>1</sup> T. Kawano,<sup>1</sup> P. Talou,<sup>1</sup> R. Capote,<sup>2</sup> and A. Trkov<sup>2</sup>

<sup>1</sup>Los Alamos National Laboratory, Los Alamos, NM 87545, USA

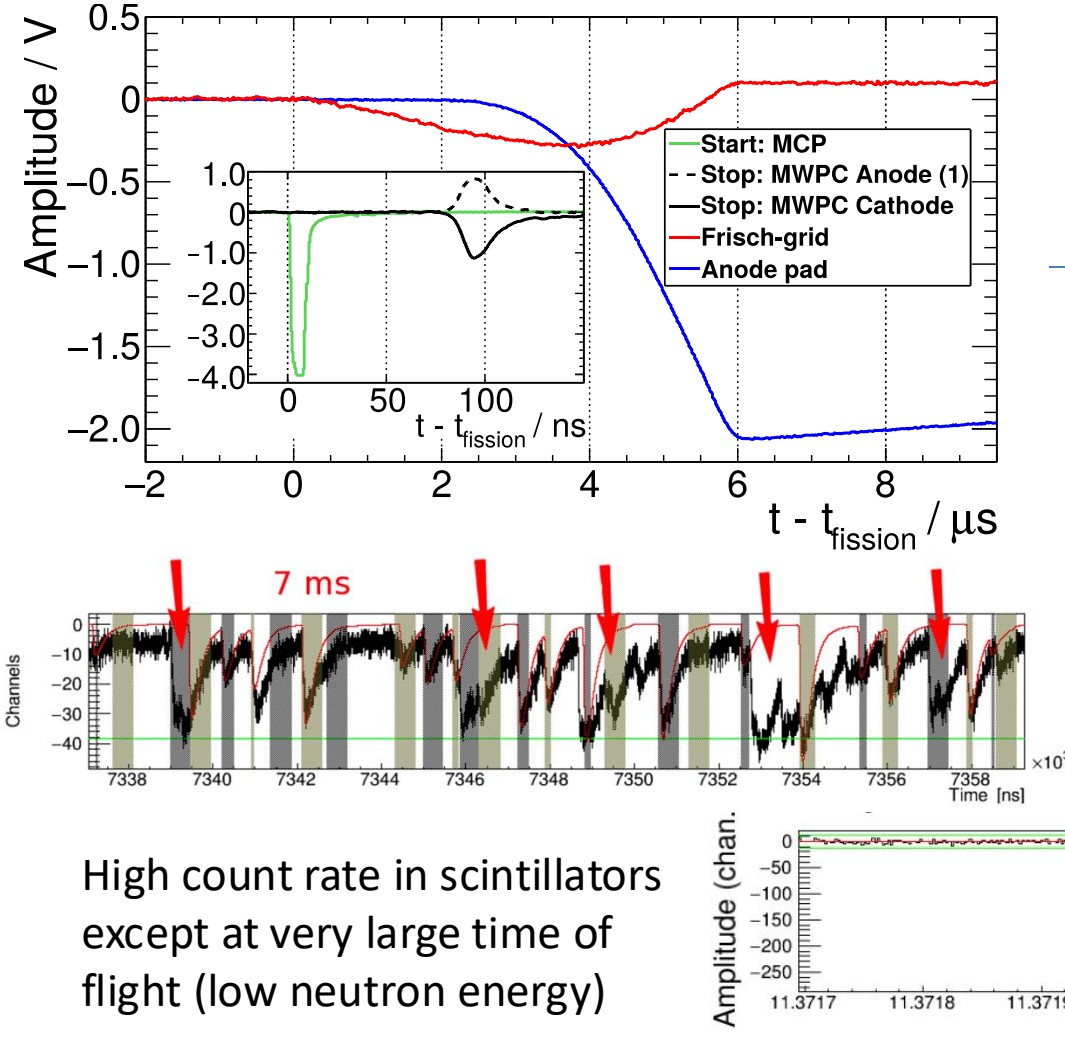
<sup>2</sup>International Atomic Energy Agency, Vienna-A-1400, PO Box 100, Austria

(Received 2 April 2019; revised received 19 July and 15 August 2019; accepted 17 August 2019)

TABLE I. Evaluation of prompt fission gamma-ray properties for  $^{235}\text{U}(n_{\text{th}},\text{f})$ : comparison between the current evaluations, experimental data and CGMF calculations. We present the average gamma multiplicity,  $\langle\nu_\gamma\rangle$ , the average gamma-ray energy,  $\langle\varepsilon_\gamma\rangle$ , and the total prompt gamma energy released,  $\langle E_\gamma^{tot} \rangle$ . All energies are in MeV. Similar time coincidence windows have been employed in all experiments included in this compilation, ranging from 6 to 10 ns. The current table is an updated version of Table XXIII in Ref. [1].

	$E_{\text{thresh}}$	$\langle\nu_\gamma\rangle$	$\langle\varepsilon_\gamma\rangle$	$\langle E_\gamma^{tot} \rangle$
ENDF/B-VIII.0	0	8.58	0.85	7.28
ENDF/B-VII.1		7.04	0.94	6.60
JEFF-3.3		8.74	0.81	7.05
JENDL 4		7.43	0.94	6.96
CGMF		7.94	0.78	6.20
ENDF/B-VIII.0	0.10	8.19	0.89	7.25
ENDF/B-VII.1	0.10	6.87	0.96	6.59
Pleasonton [31]	0.09	6.51(30)	0.99(7)	6.43(30)
Oberstedt 2013 [32, 33]	0.10	8.19(11)	0.84(2)	6.92(9)
Oberstedt 2017 [34]	0.10	7.22	0.87	6.27
CGMF	0.10	7.01	0.87	6.15
ENDF/B-VIII.0	0.14	7.78	0.93	7.21
ENDF/B-VII.1	0.14	6.72	0.98	6.57
Verbinski [35]	0.14	6.7(3)	0.97(5)	6.51(30)
Oberstedt 2017 [33]	0.14	7.01(18)	0.89(4)	6.24(20)
CGMF	0.14	6.68	0.91	6.10
Chyzh [36]	0.15	7.35		8.35
Peelle [37]	0.15	7.45(35)	0.99(7)	7.18(26)
ENDF/B-VIII.0	0.40	5.47	1.21	6.60
ENDF/B-VII.1	0.40	5.30	1.17	6.17
Jandel [38]	0.40	4.92	1.20	5.89
CGMF	0.40	4.87	1.19	5.78
Valentine [39, 40]				6.53(3)

# Analysis – signal processing

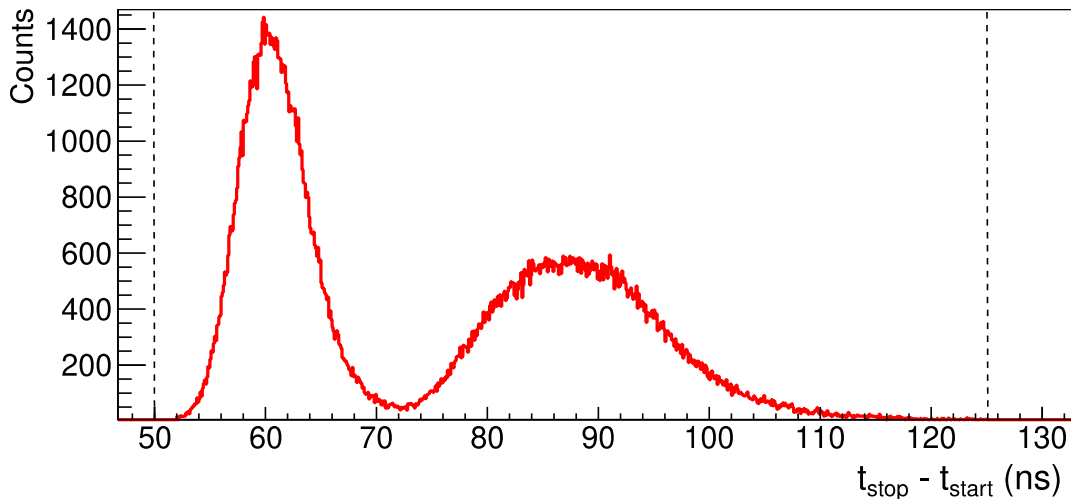


n\_TOF Pulse Shape Analysis routine  $\rightarrow$  Fission Event Builder  $\rightarrow$  Waveform analysis  $\rightarrow$  MariaDB Database

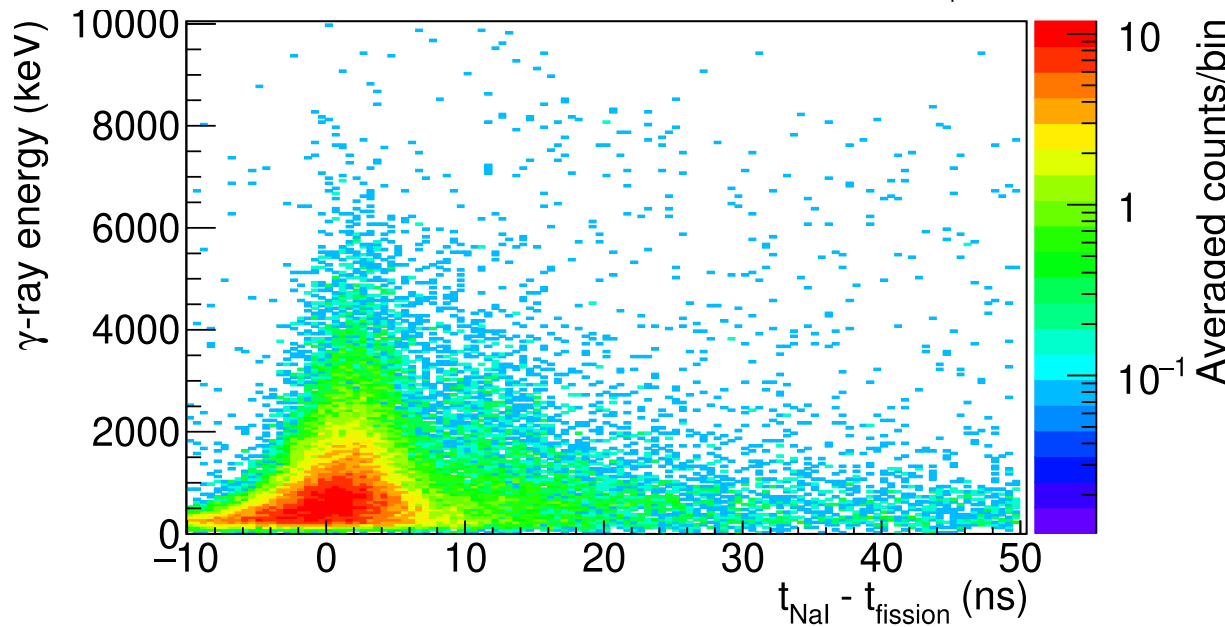
High count rate in scintillators except at very large time of flight (low neutron energy)

# Analysis – Fission Fragment Time-of-Flight and $\gamma$ -Ray Energy

---



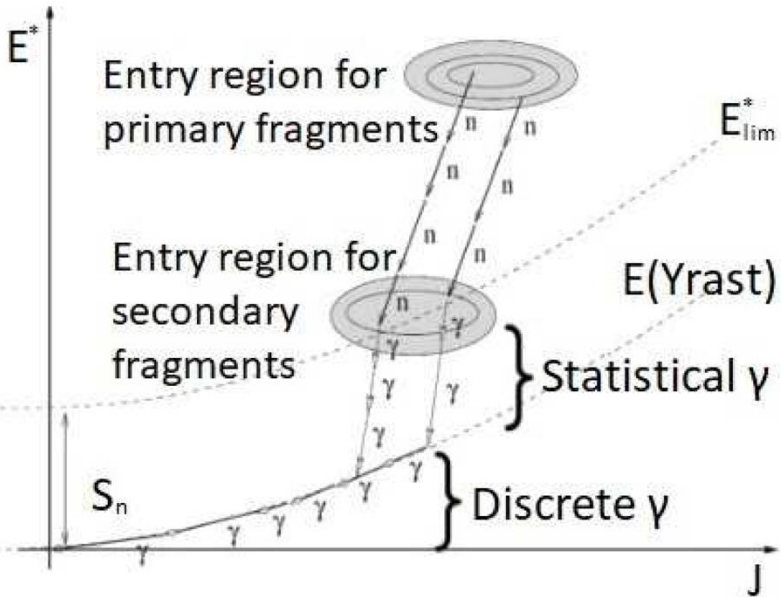
The Fission Fragment TOF spectrum. The dashed lines indicate the gate applied to identify a fission event.



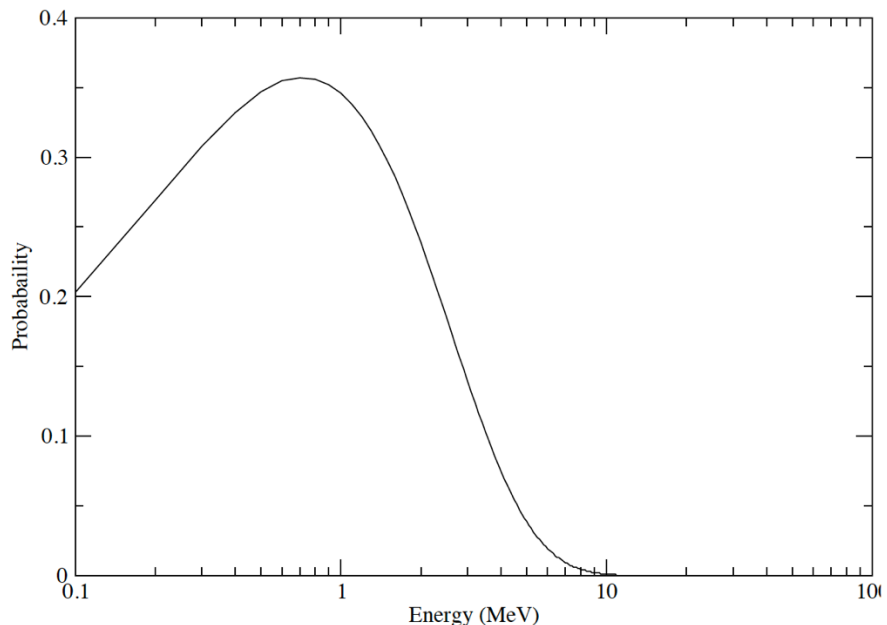
2D Histogram of  $\gamma$ -ray energy versus time detected with reference to the time of fission. The peak corresponding to prompt fission  $\gamma$ -rays is clearly visible, along with other sources of counts.

# Understanding detected $\gamma$ -ray energy: Prompt Fission Neutron Contribution

$$P(E) = a \sinh(\sqrt{2.29E}) e^{-(bE)} \text{ MeV}^{-1}$$

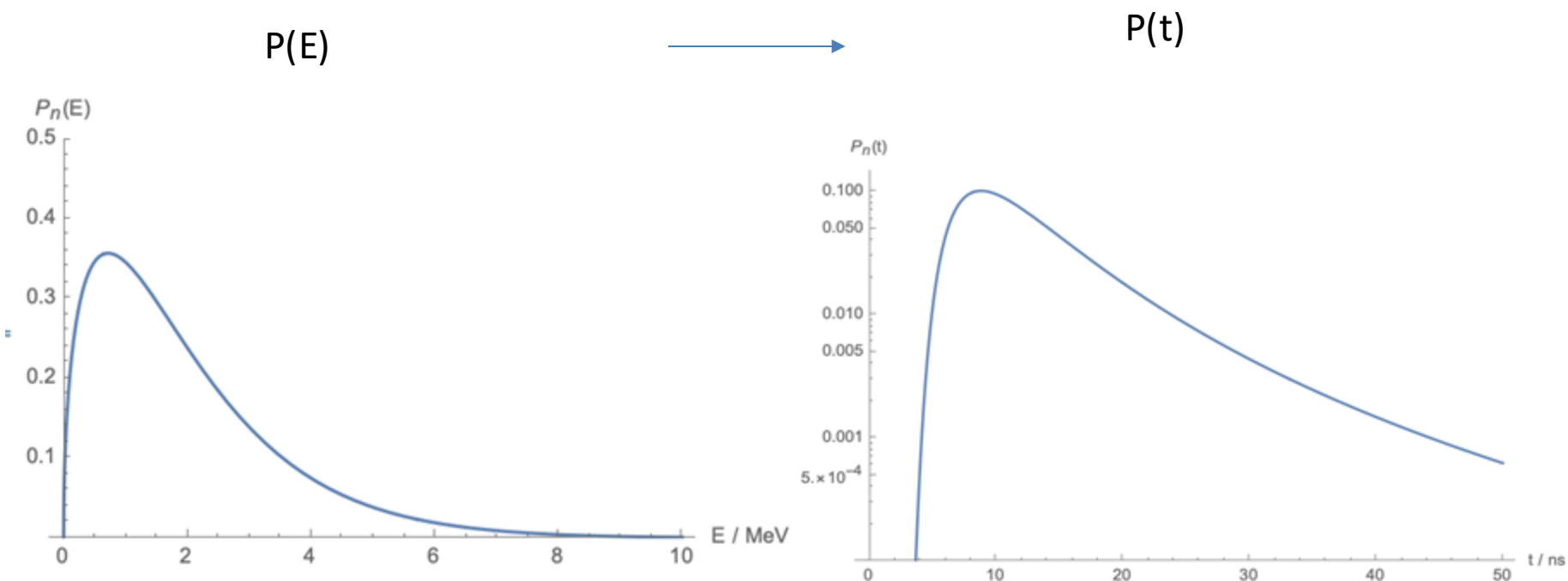


Complex situation with multiple  $\gamma$ -rays  
and neutrons emitted per fission



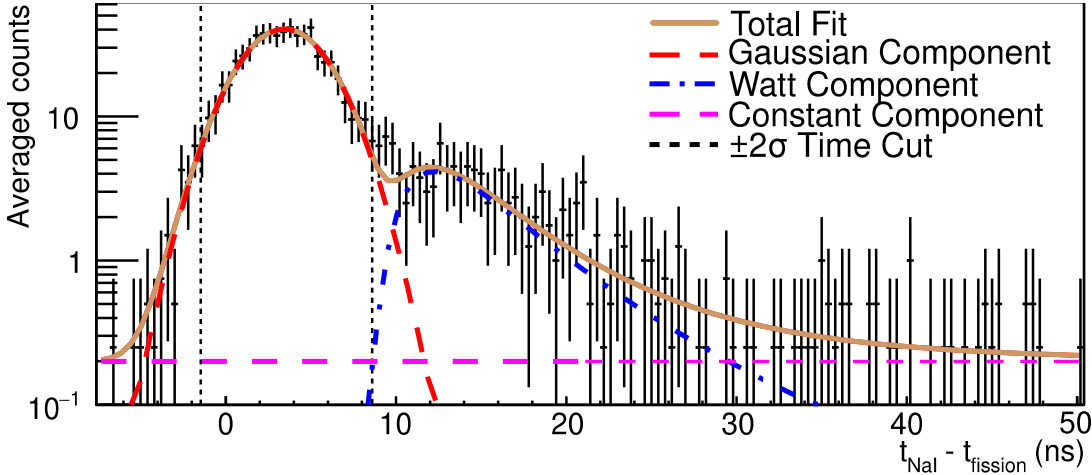
Theoretical *Watt distribution* for prompt  
fission neutron's energy distribution  
(boosted Maxwellian)

# Understanding detected $\gamma$ -ray energy: Prompt Fission Neutron Contribution



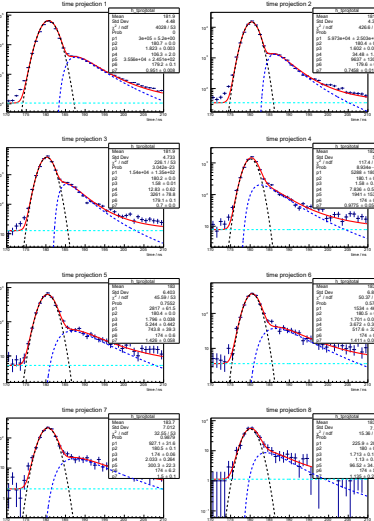
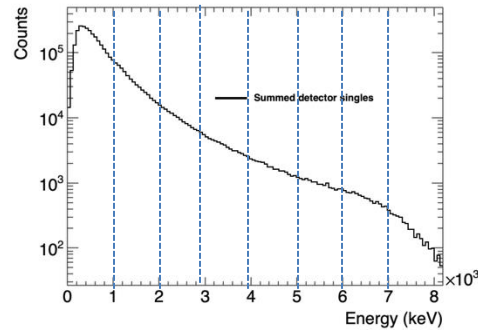
$$F(t) = \frac{a_n \sigma_n^2 e^{-\frac{208.489 \sigma_n^2}{(t - \mu_n)^2}} \sinh \left( \frac{20.42 \sigma_n}{t - \mu_n} \right)}{(t - \mu_n)^3}$$

# Understanding detected $\gamma$ -ray energy: Prompt Fission Neutron Contribution

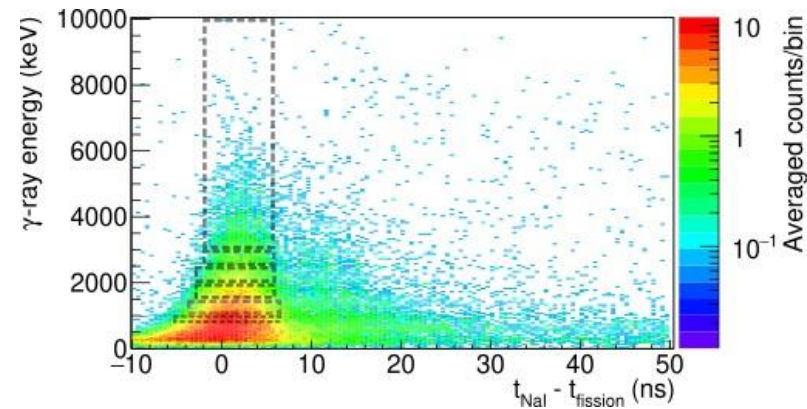


Our timing spectra contains counts around a centroid from **fission  $\gamma$ -rays following a gaussian distribution** and **neutrons following a Watt distribution** and a **constant background**.

- How do the various contributions change with  $\gamma$ -ray energy?



Perform fit for different  $\gamma$ -ray energy regions.



Need to average detectors to achieve statistics

# Understanding detected $\gamma$ -ray energy: Prompt Fission Neutron Contribution

Can estimate contribution in timing spectrum from neutrons.

- Use narrow (2 sigma) cut in time to reduce background to negligible levels
- Use wide cut in time to include all counts

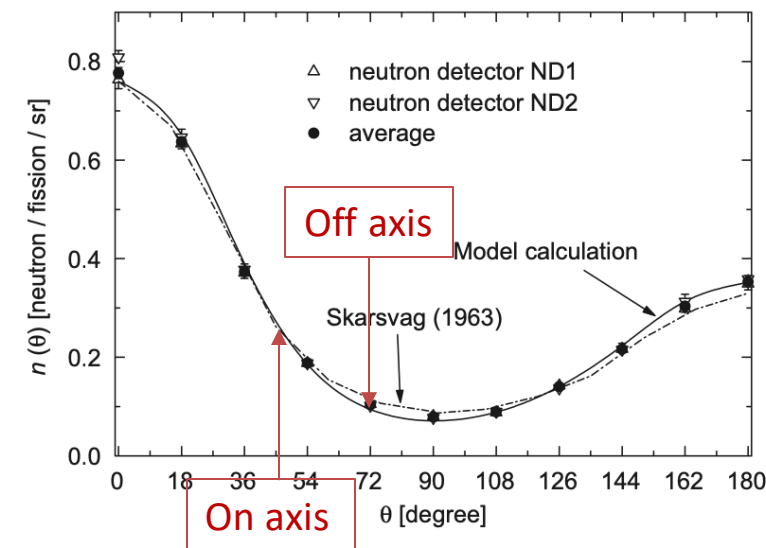
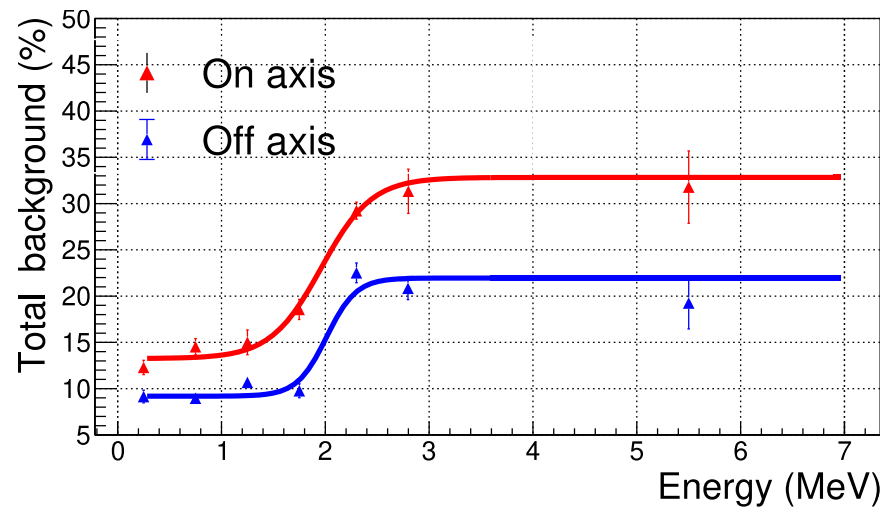


Fig. 7. Fission neutron yield as a function of the angle between neutron exit direction and the direction of motion of the light fragments.

Two methods agree within 1/2% for the mean energy and multiplicity respectively



# Understanding detected $\gamma$ -ray energy: Anisotropy correction

PHYSICAL REVIEW

VOLUME 133, NUMBER 3B

10 FEBRUARY 1964

## Directional Correlation of Fission Fragments and Prompt Gamma Rays Associated With Thermal Neutron Fission\*†

MARVIN M. HOFFMAN

*Los Alamos Scientific Laboratory, Los Alamos, New Mexico*

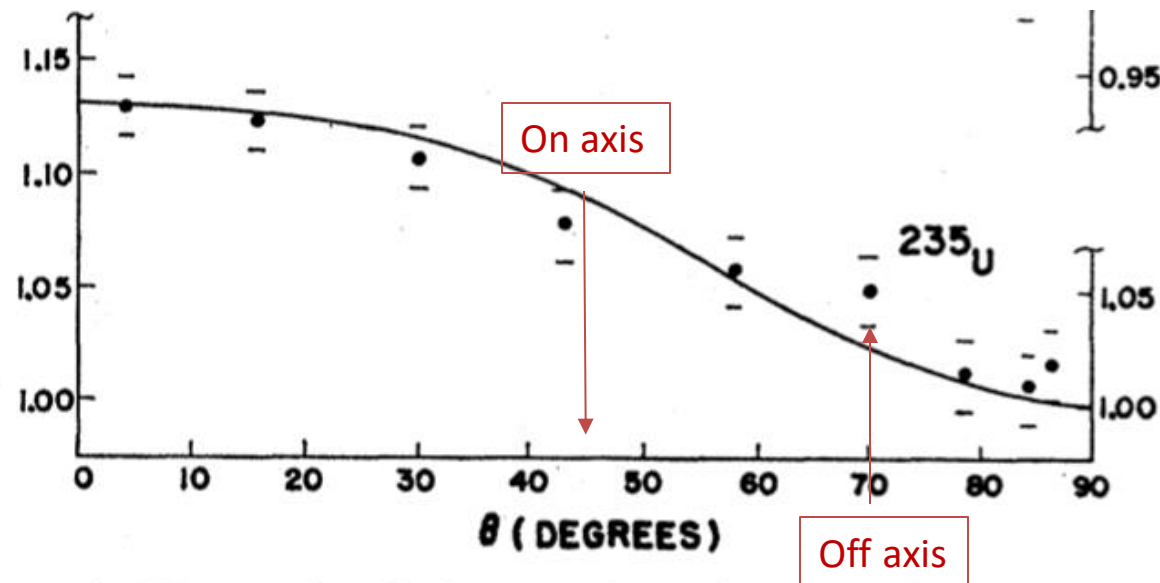
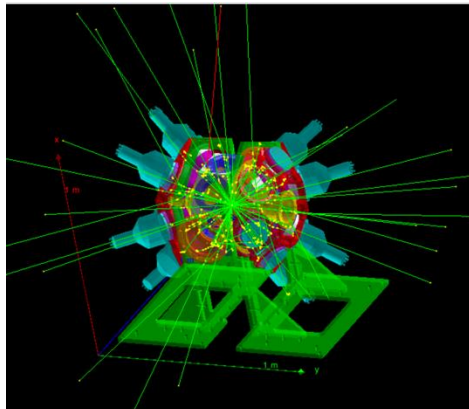


FIG. 4. Measured relative number of  $\gamma$  rays having energy greater than 250 keV as a function of the angle to the fragment direction. The solid curves are the results of a least-squares fit of

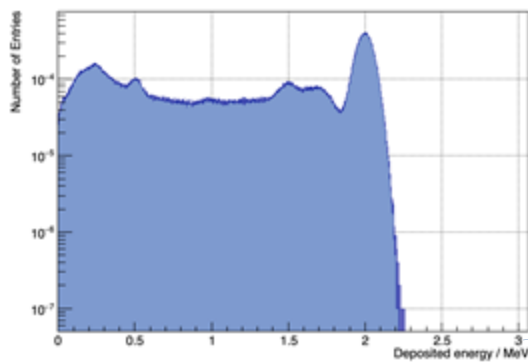
On axis measure  
~1.5% higher than  
the mean, off axis  
measure ~4.5%  
lower

Final correction  
before averaging  
all detectors

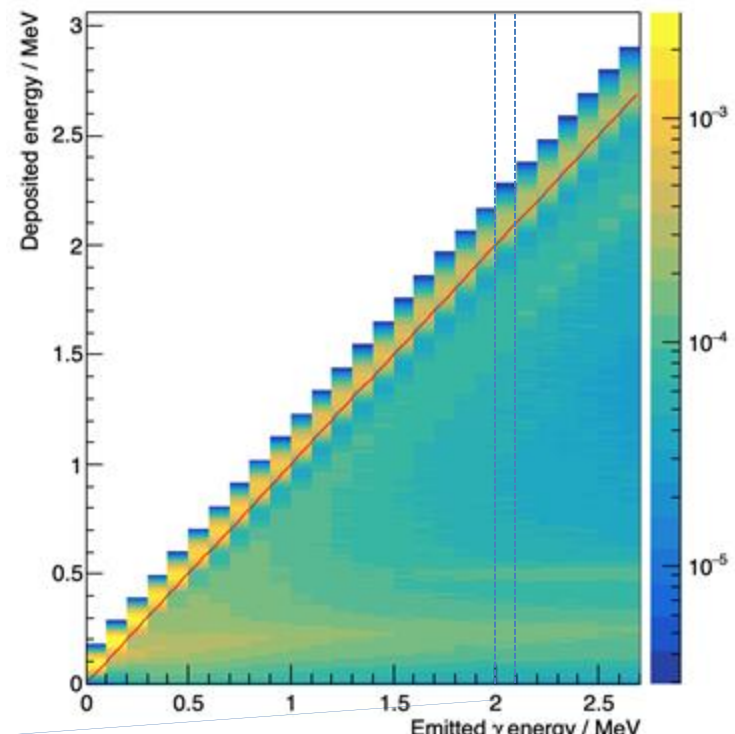
# Measured -> Emitted $\gamma$ -ray energy: Deconvolution



Geant4  
simulation of  
the STEFF  
array

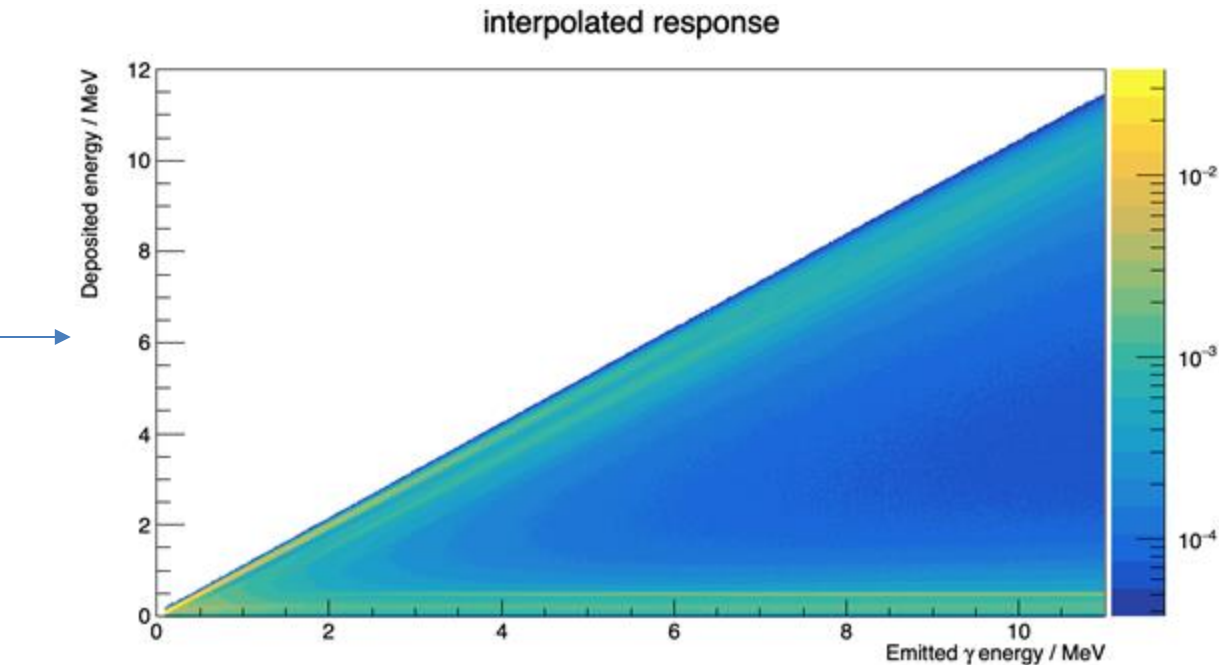
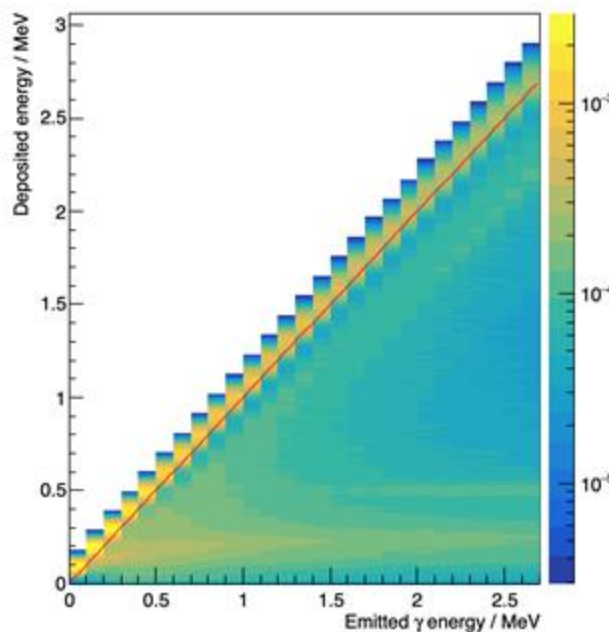


Simulated  
response to 2  
MeV  $\gamma$ -ray



Response matrix

# Measured $\rightarrow$ Emitted $\gamma$ -ray energy: Deconvolution



100 keV coarse  
response matrix



1 keV smooth  
response matrix

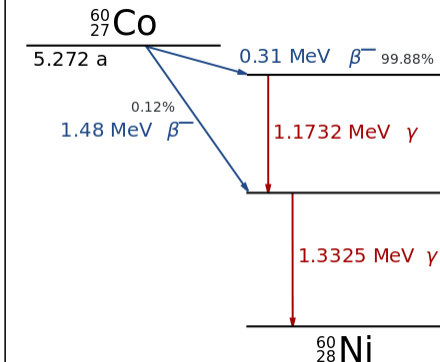
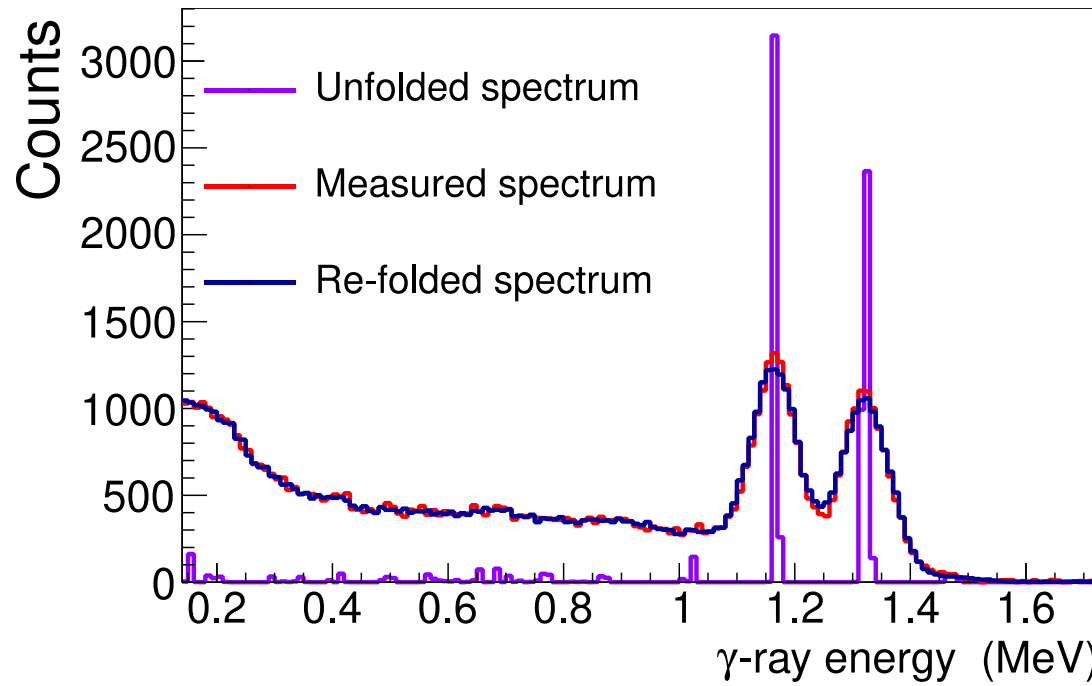
# Measured -> Emitted $\gamma$ -ray energy: Deconvolution - Gold method

'Gold'  
deconvolution  
algorithm

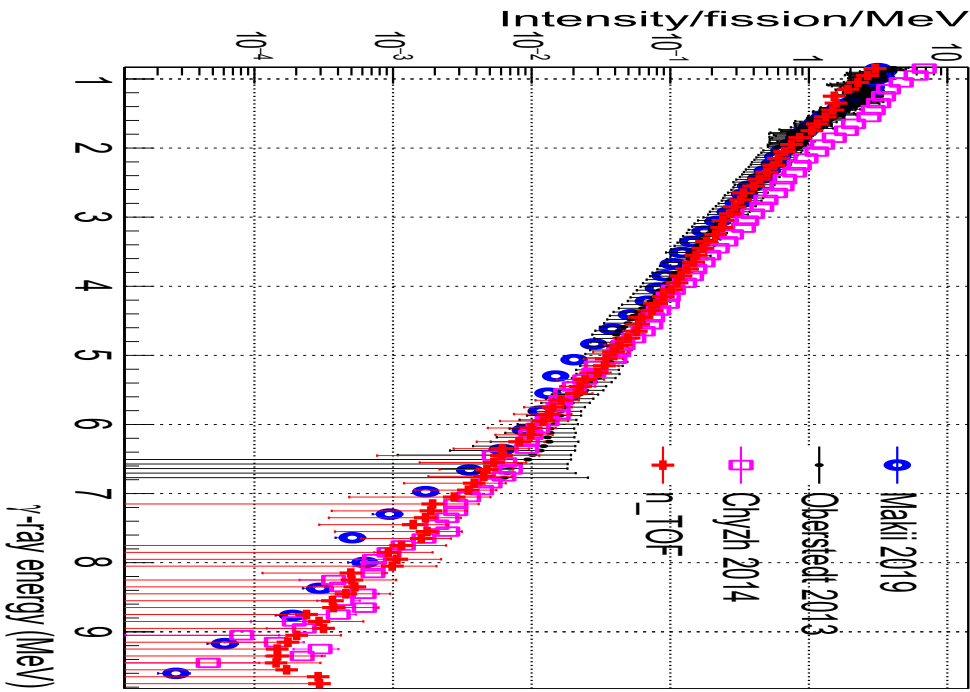
$$x^{(n+1)}(i) = \frac{y'(i)}{\sum_{m=0}^{M-1} A_{im} x^{(n)}(m)} x^{(n)}(i) \quad x^{(0)} = [1, 1, \dots, 1]^T$$

Jandl, M., Morháč, M., Kliman, J., Krupa, L., Matoušek, V., Hamilton, J.H., Ramayya, A.V.: Decomposition of continuum  $\gamma$ -ray spectra using synthesized response matrix. Nuclear Instruments and Methods in Physics Research Section A: Accelerators, Spectrometers, Detectors and Associated Equipment **516**(1), 172–183 (2004). <https://doi.org/10.1016/j.nima.2003.07.047>

Validate the  
response  
matrix



# Results



[1] Oberstedt, A., Belgya, T., Billnert, R., Borcea, R., Bryś, T., Geerts, W., Göök, A., Hambisch, F.-J., Kis, Z., Martinez, T., Oberstedt, S., Szentmiklosi, L., Takács, K., Vidali, M.: Improved values for the characteristics of prompt-fission  $\gamma$ -ray spectra from the reaction  $^{235}\text{U}(n_{\text{th}}, f)$ . Phys. Rev. C **87**, 051602 (2013). <https://doi.org/10.1103/PhysRevC.87.051602>

[2] Chyzh, A., Wu, C.Y., Kwan, E., Henderson, R.A., Bredeweg, T.A., Haight, R.C., Hayes-Sterbenz, A.C., Lee, H.Y., O'Donnell, J.M., Ullmann, J.L.: Total prompt  $\gamma$ -ray emission in fission of  $^{235}\text{U}$ ,  $^{239,241}\text{Pu}$ , and  $^{252}\text{Cf}$ . Phys. Rev. C **90**, 014602 (2014). <https://doi.org/10.1103/PhysRevC.90.014602>

**Table 1** The resulting values of  $\bar{E}_\gamma$ ,  $\bar{\nu}_\gamma$  and  $\bar{E}_\gamma \times \bar{\nu}_\gamma$  in this work compared to other recent measurements over a common energy region of 0.8 to 6.8 MeV. The uncertainties on the n\_TOF results include both statistical and systematic contributions; for the other data sets, the fractional uncertainties from their published results have been used to estimate the uncertainty in this energy range. No correlation has been included in the calculation of the  $\bar{E}_\gamma \times \bar{\nu}_\gamma$  uncertainty.

Reference	$\bar{E}_\gamma$ (MeV)	$\bar{\nu}_\gamma$	$\bar{E}_\gamma \times \bar{\nu}_\gamma$ (MeV)
Oberstedt <i>et al.</i> [1]	1.64(4)	2.99(4)	4.9(1)
Chyzh <i>et al.</i> [2]	1.56(4)	3.24(15)	5.1(3)
Makii <i>et al.</i> [3]	1.56(4)	3.04(7)	4.7(2)
n_TOF	1.71(5)	2.66(18)	4.54(3)

Recent measurements in agreement  
within uncertainties (up to 7%)  
therefore HPRL entry satisfied

[3] Makii, H., Nishio, K., Hirose, K., Orlandi, R., Léguillon, R., Ogawa, T., Soldner, T., Köster, U., Pollitt, A., Hambisch, F.-J., Tsekhanovich, I., Aïche, M., Czajkowski, S., Mathieu, L., Petrache, C.M., Astier, A., Guo, S., Ohtsuki, T., Sekimoto, S., Takamiya, K., Frost, R.J.W., Kawano, T.: Effects of the nuclear structure of fission fragments on the high-energy prompt fission  $\gamma$ -ray spectrum in  $^{235}\text{U}(n_{\text{th}}, f)$ . Phys. Rev. C **100**, 044610 (2019). <https://doi.org/10.1103/PhysRevC.100.044610>

# Acknowledgements

---

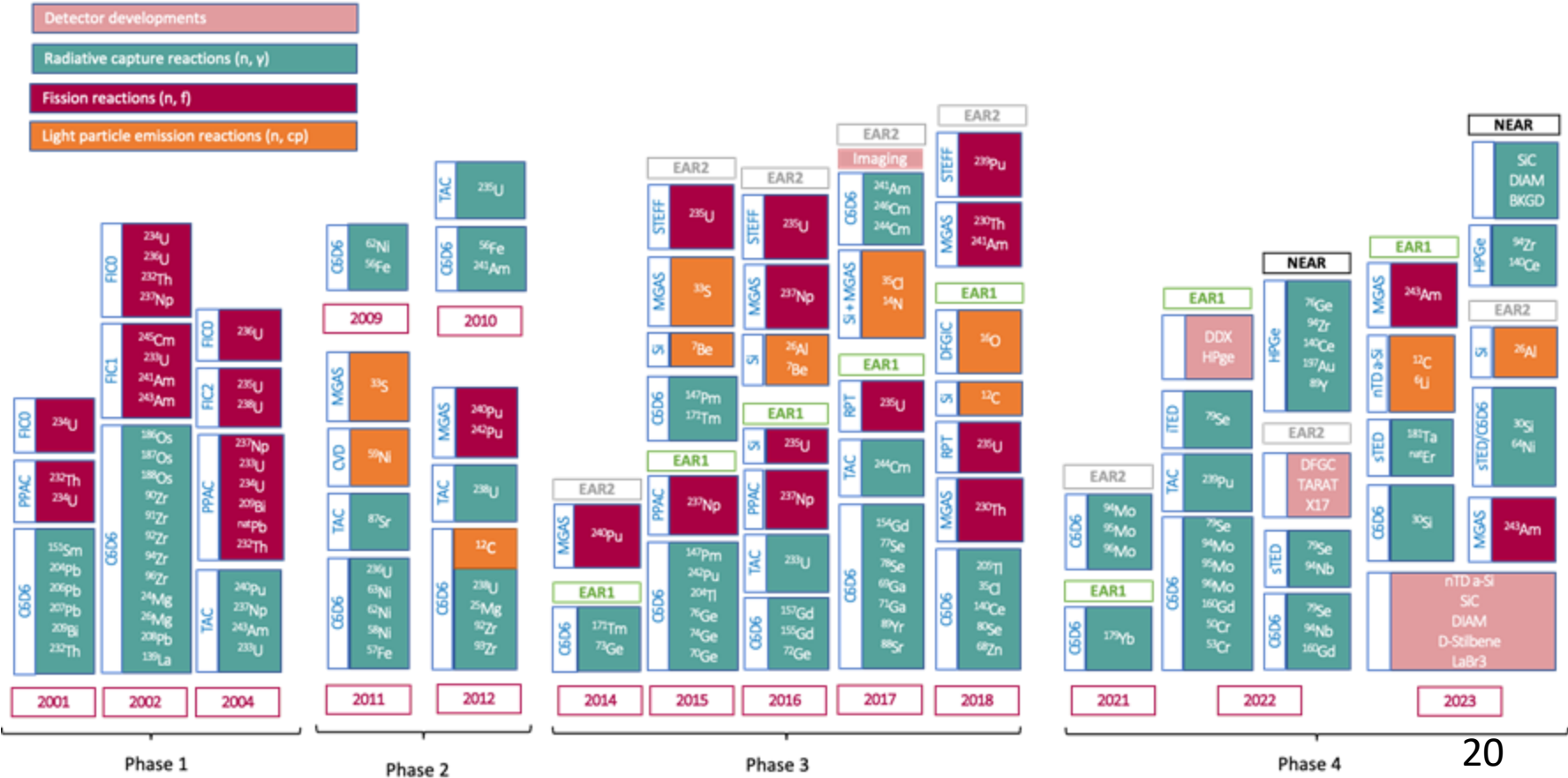
- University of Manchester team:
  - Prof. Gavin Smith
  - Dr Nikolay Sosnin
  - Dr Sam Bennett
  - Dr Paul Davies (now University of York)
  - Dr Adhitya Sekhar
  - Vlad Popescu
- The n\_TOF collaboration



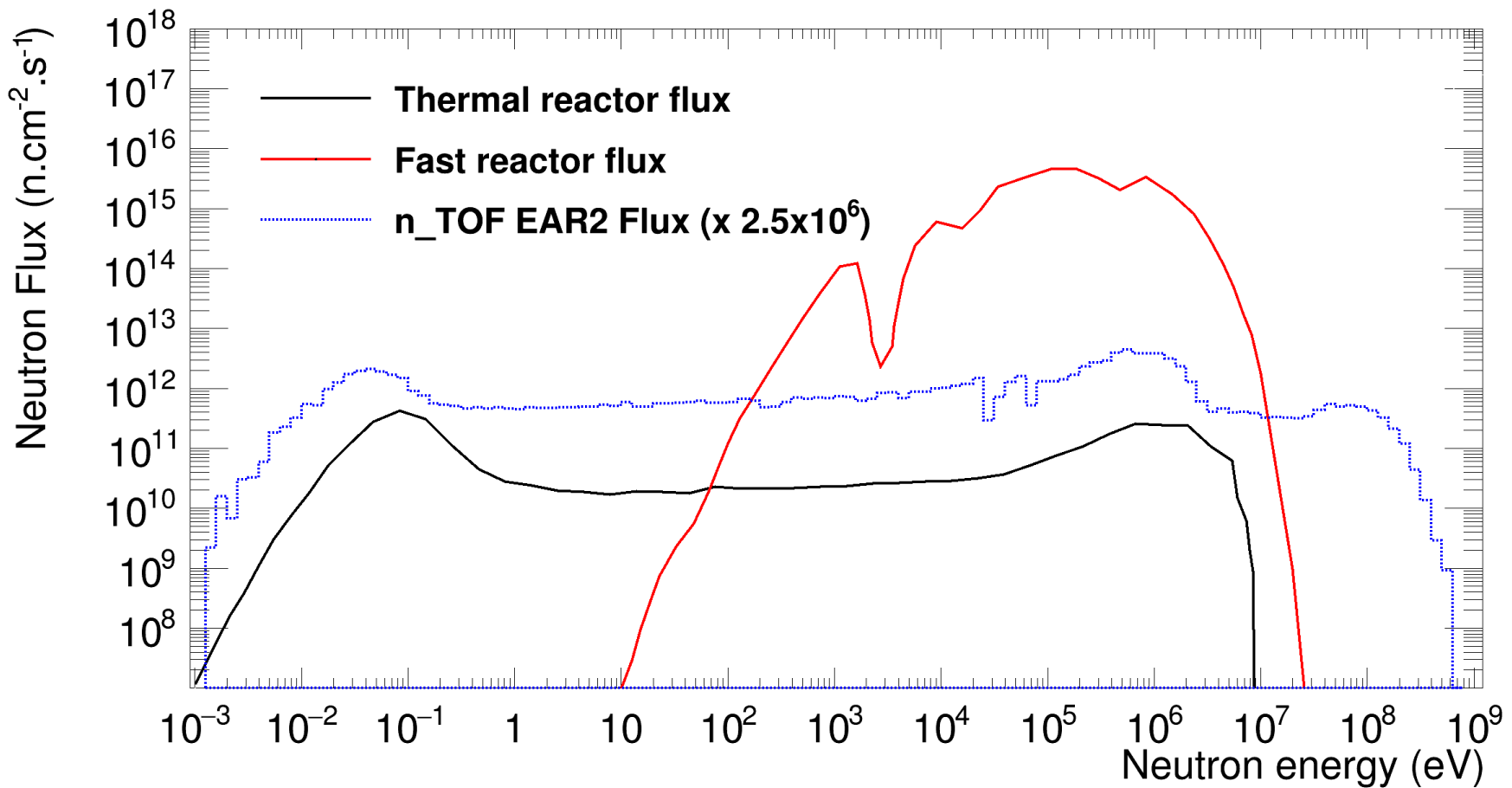
The University of Manchester



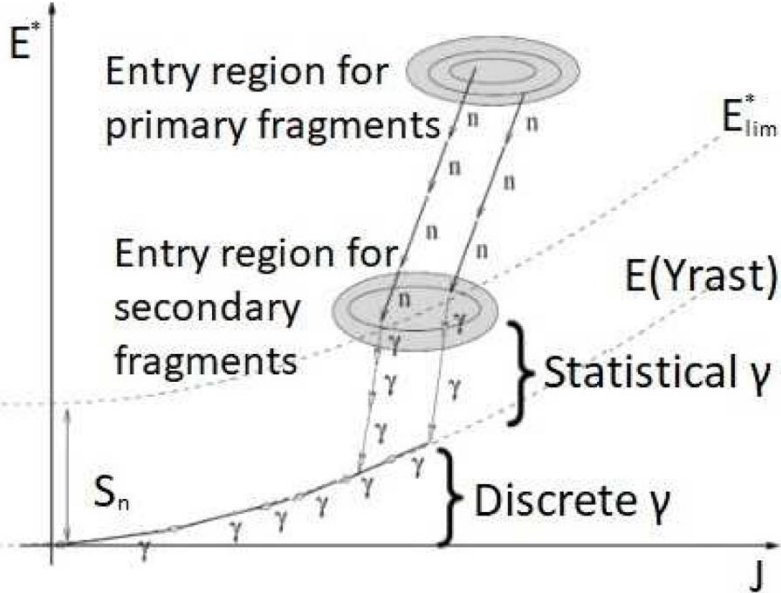
# The n\_TOF history in a nutshell



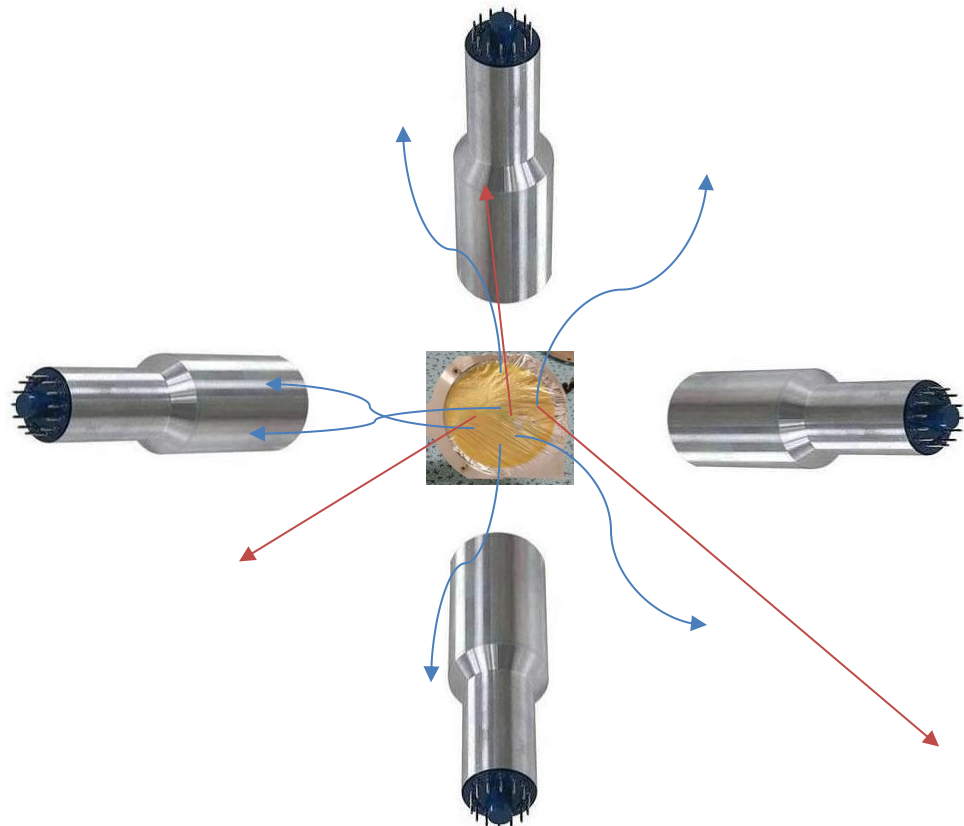
# The n\_TOF facility



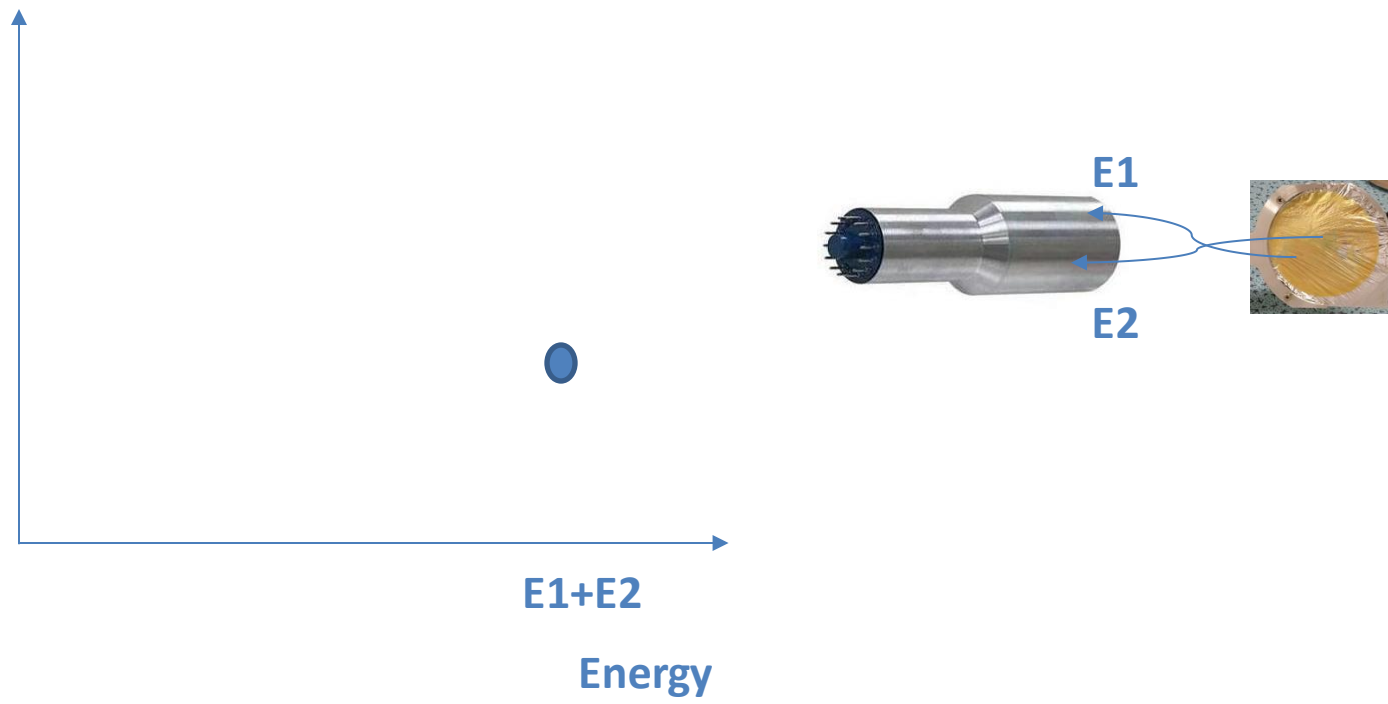
# Detected $\gamma$ -rays – understanding their origin



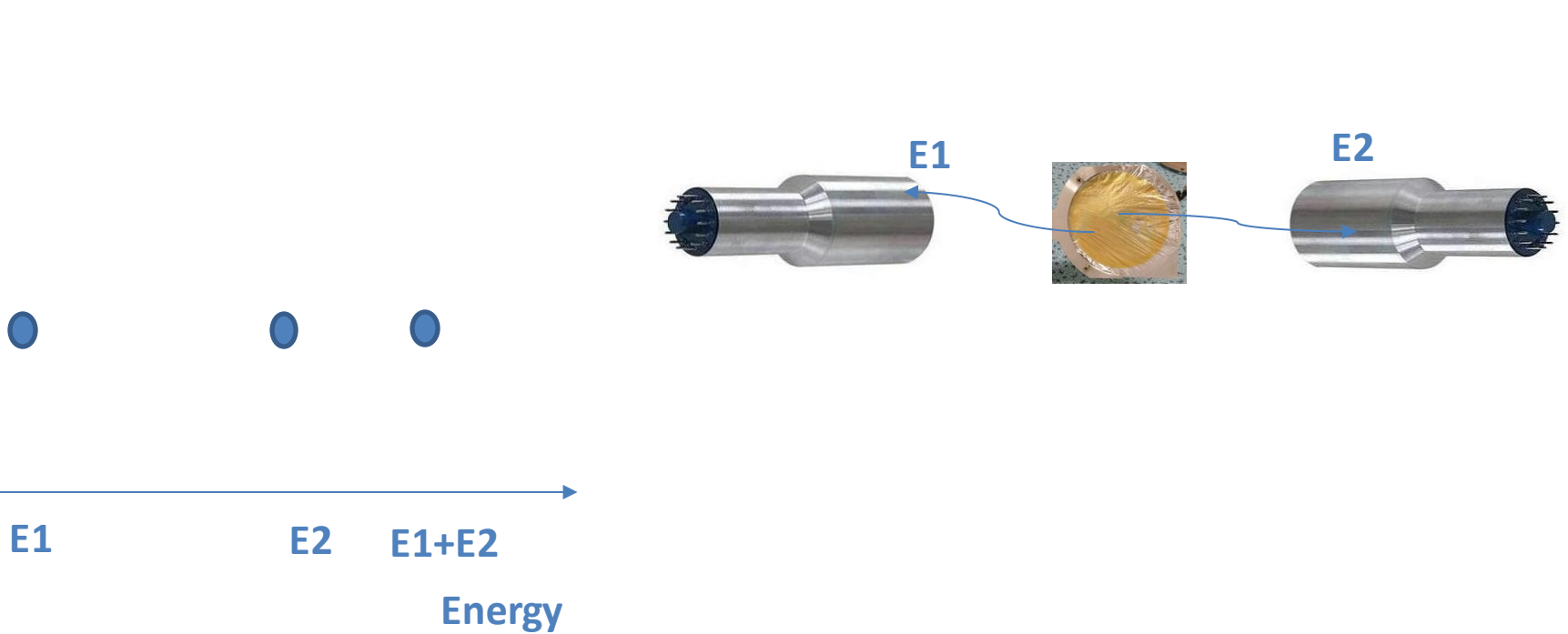
Complex situation with multiple  $\gamma$ -rays  
and neutrons emitted per fission



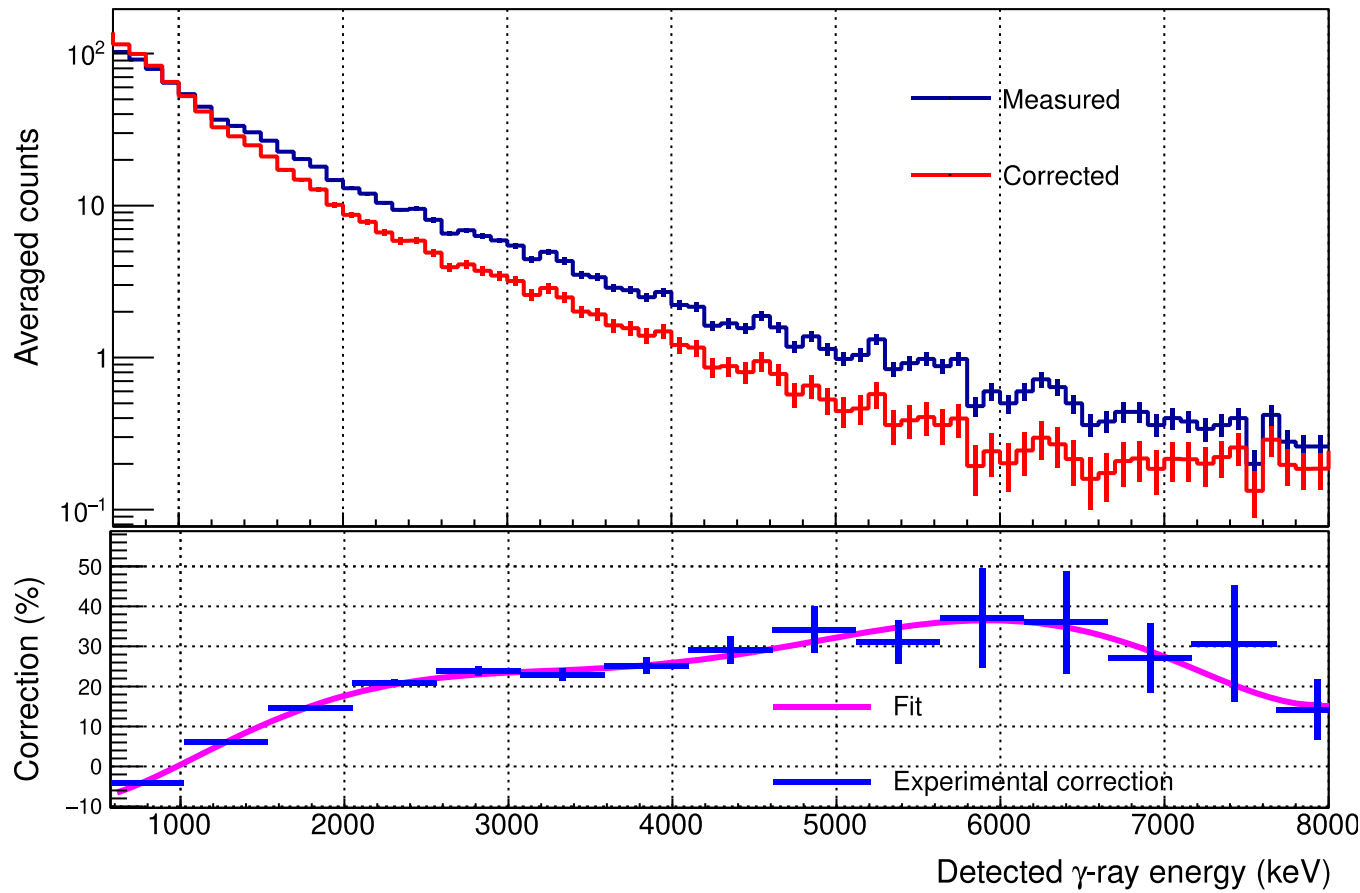
# Understanding detected $\gamma$ -ray energy: Multiple hits correction



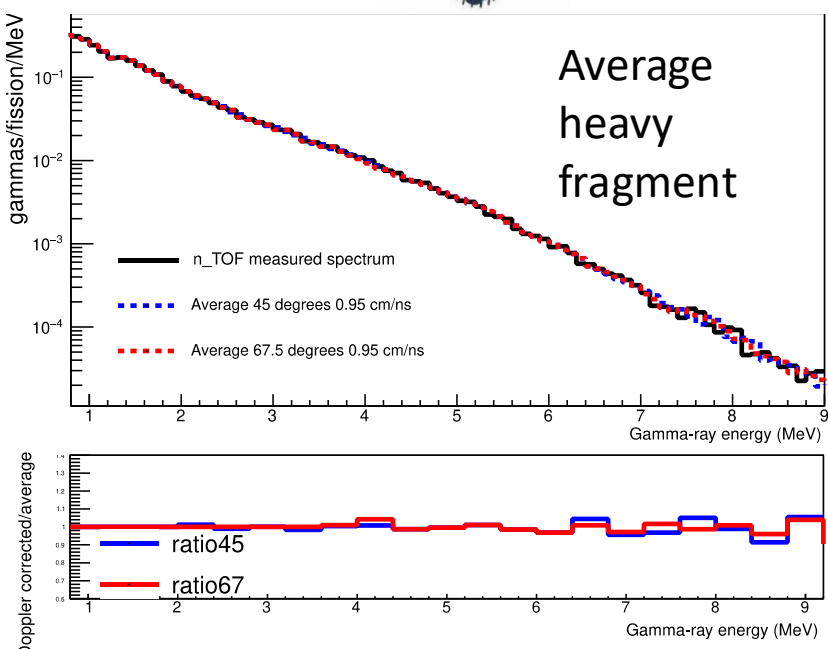
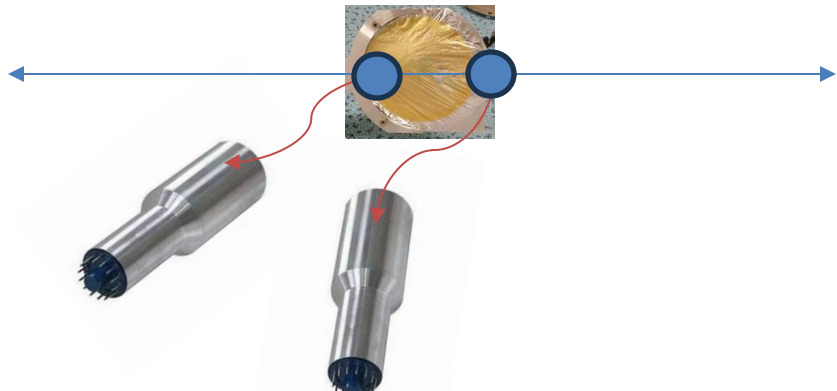
# Understanding detected $\gamma$ -ray energy: Multiple hits correction



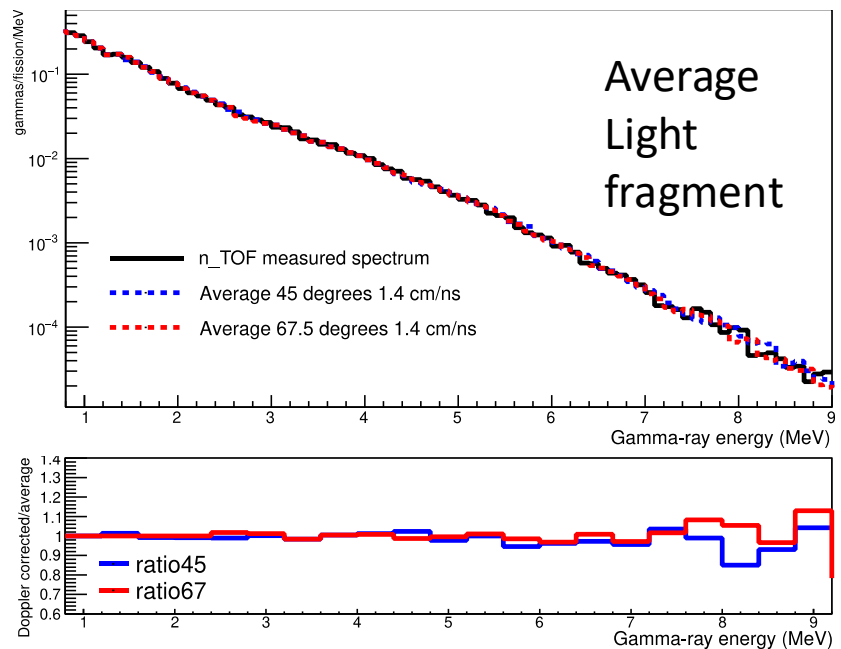
# Understanding detected $\gamma$ -ray energy: Multiple hits correction



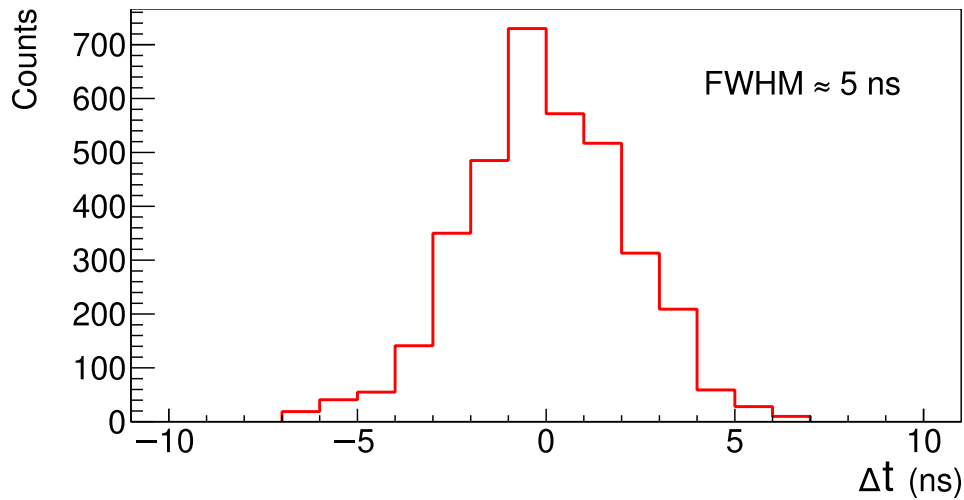
# Understanding detected $\gamma$ -ray energy: Doppler correction



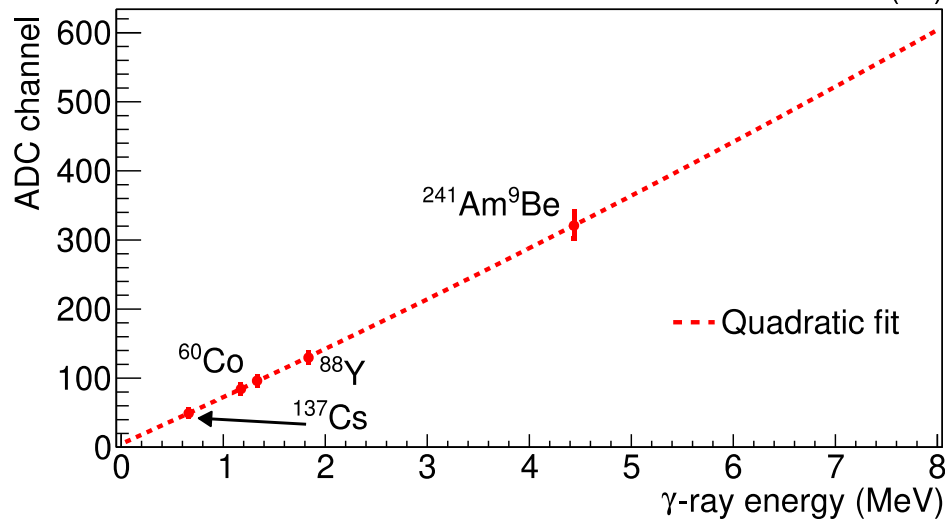
$$E'_\gamma = \frac{E_\gamma}{\gamma(1 + \beta \cos\theta)}$$



# Analysis – NaI Calibration



The time  $\Delta t$  between signals in different detectors corresponding to detected photo-peak  $\gamma$ -rays from a  $^{60}\text{Co}$  source for a single NaI detector within the array. These  $\gamma$ -rays are emitted simultaneously, thus the measured distribution in time shows our intrinsic timing resolution.



Energy calibration for the same NaI detector. The quadratic fit is shown with a dashed line. The error bars on the data points represent full-width half-maxima of the  $\gamma$ -ray peaks.

# Start only ( $\text{LaBr}_3$ )

---

